ResearchGate

See discussions, stats, and author profiles for this publication at: https://www.researchgate.net/publication/299975978

Stabilization of a Quadrotor With Uncertain Suspended Load Using Sliding Mode Control

Conference Paper · August 2016

DOI: 10.1115/DETC2016-60060

CITATIONS
0

READS
195

4 authors, including:

Xu Zhou
Colorado School of Mines
1 PUBLICATION **0** CITATIONS
SEE PROFILE

Rui Liu
Colorado School of Mines
13 PUBLICATIONS **37** CITATIONS
SEE PROFILE

Some of the authors of this publication are also working on these related projects:

NL-supported Manufacturing View project

Robot Cognition View project

All content following this page was uploaded by Xu Zhou on 05 August 2016.

The user has requested enhancement of the downloaded file. All in-text references underlined in blue are added to the original document and are linked to publications on ResearchGate, letting you access and read them immediately.

**ASME 2016 International Design Engineering Technical Conferences &
Computers and Information in Engineering Conference
IDETC2016
August 21-24, 2016, Charlotte, North Carolina, USA**

IDETC2016-60060

STABILIZATION OF A QUADROTOR WITH UNCERTAIN SUSPENDED LOAD USING SLIDING MODE CONTROL

Xu Zhou
Colorado School of Mines
Golden, Colorado, USA

Rui Liu
Colorado School of Mines
Golden, Colorado, USA

Jiucai Zhang
National Renewable Energy Laboratory
Golden, Colorado, USA

Xiaoli Zhang
Colorado School of Mines
Golden, Colorado, USA

ABSTRACT

The stability and trajectory control of a quadrotor carrying a suspended load with a fixed known mass has been extensively studied in recent years. However, the load mass is not always known beforehand in practical applications. This mass uncertainty brings uncertain disturbances to the quadrotor system, causing existing controllers to have a worse performance or to be collapsed. To improve the quadrotor's stability in this situation, we investigate the impacts of the uncertain load mass on the quadrotor. By comparing the simulation results of two controllers -- the proportional-derivative (PD) controller and the sliding mode controller (SMC) driven by a sliding mode disturbance of observer (SMDO), the quadrotor's performance is verified to be worse as the uncertainty increases. The simulation results also show a controller with stronger robustness against disturbances is better for practical applications.

1. INTRODUCTION

Aerial load transportation has recently received considerable attentions as an important application of the physical interaction between unmanned aerial vehicles (UAVs) and the surrounding environment [1, 2]. Specifically, quadrotor UAVs can play an important role in delivering loads to some dangerous or hardly inaccessible places due to their simple mechanical structures as well as desirable hovering and vertical take-off and landing (VTOL) capabilities [3-7]. Even though the quadrotor load transportation is promising, it is still very challenging in real situations. One reason is the quadrotor itself is an underactuated system. With only four inputs with six degrees of freedom (DOF) to control, the quadrotor is easily unstable and inherently difficult to control. Another difficulty is suspended loads can change the quadrotor's own dynamics, thereby bringing external disturbances into the quadrotor model. This could also potentially cause existing model-based controllers to have decreased performance or even collapse. These open challenges limit the stability performance of quadrotor load transportation and therefore hinder its adaption in practical applications.

With the help of the quadrotor's popularity, some researchers have started solving these challenges in certain load transportation, i.e. the quadrotor with a fixed known load. Their work mainly investigated the quadrotor's stability and trajectory tracking performances. For example, [3, 4] generated and tracked swing-free trajectories by utilizing the dynamic programming algorithm. A novel coordinate-free form for dynamic motion equations was developed in [5], which was suitable for robot control system design. A geometric nonlinear controller was also presented to asymptotically stabilize the whole system. [8] proved a quadrotor with a cable-suspended load system to be differentially-flat and proposed a nonlinear control method to track the trajectory in a two-dimensional plane. The extension of this method for 3D cases was given in [9]. The change of a quadrotor's center of gravity (CoG) caused by the swing load was dealt with by an adaptive controller in [10]. In [11], more challenging trajectory tracking such as passing through a small window without prior knowledge of the window position was obtained using an iterative Linear-Quadratic-Gaussian algorithm. [12] presented a new motion planning method by generating trajectories with minimal residual oscillations through a finite-sampling, batch reinforcement learning technique. [13] explored the safe and precise operation of the quadrotor with a heavy slung load through a novel nonlinear model predictive controller. In [6, 7, 14-16], the situation in which multiple quadrotors working together to transport a cable suspended load in a three-dimensional space was studied.

Copyright © 2016 by ASME

However, the practical load mass information could be completely uncertain beforehand [17, 18]. From the quadrotor's perspective, this load uncertainty results in a correspondingly uncertain external disturbance. If the controller is not robust against external disturbances, then the quadrotor's stability could be notably affected. This vulnerability is unacceptable considering the real application needs a stable load transportation method. To render the quadrotor load transportation practically useful, there is a fundamental need to both understand the influence of the load mass uncertainty and develop a controller to better deal with this uncertainty.

Few works have been reported for the quadrotor transporting uncertain loads. [17] treated the uncertain load as a parametric model uncertainty and developed an adaptive robust controller to compensate for this uncertainty. However, the load in [17] was assumed to be attached to the quadrotor directly, which makes the dynamic model less complex than that of a suspended one. Therefore, the method in [17] may not be considered to apply in the suspended load situation. By treating the uncertain load mass as a nominal mass plus an uncertainty, [18] proposed a fixed-gain nonlinear proportional-derivative (PD) controller for the nominal one and designed another retrospective adaptive controller to compensate for the uncertainty. However, this compensation was considered in only altitude direction. Since the load mass uncertainty affects more than altitude motion, this compensation design may limit its practical applications. More importantly, both [17] and [18] did not clearly investigate the vital influence of the uncertain load on the quadrotor.

In this work, our goal is to improve the quadrotor's stability under the influences of uncertain suspended load masses. In order to achieve this goal, we need to understand how the load mass uncertainty impacts the quadrotor's stability. For the summarization of this understanding, we evaluate the performances of two controllers -- the PD controller and the sliding mode controller (SMC) driven by a sliding mode disturbance of observer (SMDO). Although some SMC related controllers have been done for the quadrotor [19-22], they are only designed for the quadrotor itself. In this work, we modified this advanced method accordingly so that we can apply it into a new scenario, i.e. a quadrotor with a suspended load, to get a comparison. In short, our main contributions include: (1) In terms of the stabilization time and attitude angle overshoot, investigate the impacts of the uncertain load on the quadrotor. The quadrotor's stability is proved to be worse as the uncertainty increases. (2) Verify that a controller with strong robustness against disturbances is a better choice for the quadrotor carrying an uncertain suspended load. The better performance of SMDO-SMC than a conventional PD controller supports this conclusion.

2. MATHEMATICAL MODELING

The controller design should be based on a realistic dynamic model so that the design can be evaluated judicially. Therefore, in this section, we focus on the development of a realistic and comprehensive dynamic model of this interconnected system.

2.1 Assumptions

Mathematical models are of great importance for the quadrotor control. Without violating the correctness of the final result, we can make the following assumptions to help us simplify the dynamic modeling [23].

1) The quadrotor body is rigid and symmetrical.
2) The quadrotor's center of gravity is coincided with the body fixed frame origin.
3) The suspension point is exactly the quadrotor's center of gravity.
4) The cable is massless and the cable force is always non-negative and non-negligible.
5) There are no other external disturbances or interactions, such as wind gust, to the quadrotor except for the load.

These assumptions are considered to be sufficient and valid for the realistic representation of the quadrotor with a swing load system, which is used for a nonaggressive trajectory tracking [23]. With assumption (1), we can make the body fixed inertia matrix to be diagonal or, in other words, the product of inertia off the diagonal is zero. Assumptions (2) and (3) help to simplify the dynamic modeling by eliminating some unnecessary offsets to the quadrotor's center of gravity. According to assumption (4), the cable should always be taunt to ensure the load is prevented from flying into the upper hemisphere of the quadrotor. Assumption (5) rejects the highly nonlinear aerodynamic affects to ensure the load is the main influence on the quadrotor.

2.2 Quadrotor Dynamic Modeling

To derive the motion equations of a 6 DOF quadrotor, we first define two coordinate frames shown in Figure 1. Frame {W} is defined as the inertial frame (world frame) and Frame {B} is the body frame.

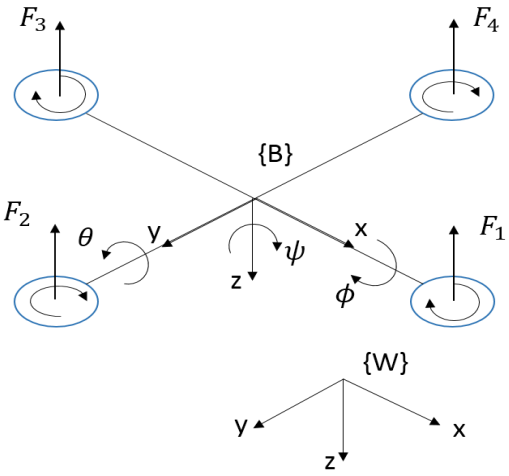

Figure 1: Schematic of Quadrotor Dynamics

Based on assumptions (1) - (2), (5) and considering the low-speed fly situation, we can derive the quadrotor dynamics as [24, 25]

$$\dot{\boldsymbol{p}} = \boldsymbol{v} \tag{1}$$

$$m_q \dot{\boldsymbol{v}} = m_q \boldsymbol{g} + \mathbf{R}\boldsymbol{f} \tag{2}$$

Copyright © 2016 by ASME

$$\dot{\mathbf{R}} = \mathbf{R}\mathbf{S}(\boldsymbol{\Omega}) \tag{3}$$

$$\mathbf{I}\dot{\boldsymbol{\Omega}} = \mathbf{S}(\mathbf{I}\boldsymbol{\Omega})\boldsymbol{\Omega} + \boldsymbol{T} \tag{4}$$

where $\boldsymbol{p} = (\mathrm{x}, \mathrm{y}, \mathrm{z})^{\mathrm{T}} \in \mathbb{R}^3$ is the quadrotor position measured in frame {W}, $\boldsymbol{v} = \dot{\boldsymbol{p}} \in \mathbb{R}^3$ is the linear translational velocity expressed in frame {W}, $\dot{\boldsymbol{v}} \in \mathbb{R}^3$ is the linear translation acceleration expressed in frame {W}, m_q is the quadrotor mass, $\boldsymbol{g} = (0,0,g)^T$ is the acceleration of gravity, $\boldsymbol{R} \in SO^3$ is a rotation matrix from the body frame {B} to the inertial frame {W}, $\boldsymbol{f}$ is upwards thrust directed along the negative body-aligned z-axis, $\boldsymbol{\Omega} \in \mathbb{R}^3$ is the angular velocity expressed in frame {B}, $\dot{\boldsymbol{\Omega}} \in \mathbb{R}^3$ is the angular acceleration expressed in frame {B}, $\mathbf{S}(\cdot)$ is the skew-symmetric operator such that $p \times q = \mathbf{S}(p)q$, $\mathbf{I} = diag\{I_x, I_y, I_z\}$ is the body-fixed inertia matrix, and $\boldsymbol{T}$ is the applied moments on quadrotor.

Extending Eqs. (1) - (4), the complete dynamic model [26, 27] is as following.

$$\begin{cases} \ddot{x} = \dfrac{(\cos\phi \sin\theta \cos\psi + \sin\phi \sin\psi)}{m_q} U_1 \\ \ddot{y} = \dfrac{(\cos\phi \sin\theta \sin\psi - \sin\phi \cos\psi)}{m_q} U_1 \\ \ddot{z} = \dfrac{\cos\phi \cos\psi}{m_q} U_1 + g \\ \ddot{\phi} = \dfrac{I_y - I_z}{I_x}\dot{\theta}\dot{\psi} + \dfrac{l}{I_x} U_2 \\ \ddot{\theta} = \dfrac{I_z - I_x}{I_y}\dot{\phi}\dot{\psi} + \dfrac{l}{I_y} U_3 \\ \ddot{\psi} = \dfrac{I_x - I_y}{I_z}\dot{\theta}\dot{\phi} + \dfrac{1}{I_z} U_4 \end{cases} \tag{5}$$

where $(\mathrm{x}, \mathrm{y}, \mathrm{z})$ are the translational displacements in x, y, and z directions, (ϕ, θ, ψ) is the angles of roll, pitch and yaw, which parameterize the orientation of frame {B} with respect to frame {W}. l is the distance between the rotor's center and the quadrotor's CoG. U_1, U_2, U_3 *and* U_4 are system inputs, which are the combinations of individual rotor thrusts, where $\boldsymbol{f} = [0, 0, U_1]$ and $\boldsymbol{T} = [U_2, U_3, U_4]$.

$$\begin{cases} U_1 = F_1 + F_2 + F_3 + F_4 \\ U_2 = -F_1 + F_3 \\ U_3 = -F_2 + F_4 \\ U_4 = Q_1 - Q_2 + Q_3 - Q_4 \end{cases} \tag{6}$$

where F_i represents thrust forces generated by four rotors, Q_i represents rotor moments. Both are proportional to the square of the angular speed.

2.3 Slung Load Modeling

From assumptions (3) and (5), we can consider the slung load as a spherical pendulum fixed at a single point. As shown in Figure 2, the origin of the load coordinate system is exactly at the quadrotor's center of gravity, and the axes are parallel to the quadrotor's axes.

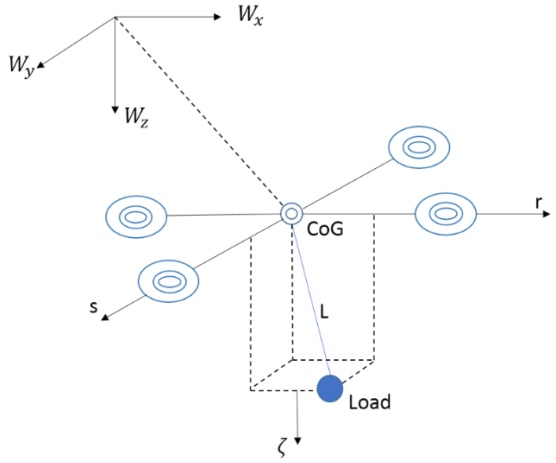

Figure 2: Schematic of quadrotor dynamics with a slung load

Because the load is not allowed to swing to the upper hemisphere above the quadrotor, we need to make sure $\zeta = \sqrt{L^2 - r^2 - s^2}$ always nonnegative. For the interconnected system, the Euler-Lagrange method [13, 28] is used to compute the load accelerations $\ddot{r}$ and $\ddot{s}$, which are shown in Eq. (8).

2.4 Coupling Dynamics Analysis

Since the suspended load has a non-negligible influence on the quadrotor, there is always a cable force between the quadrotor and load. According to the Newton's second law of motion, the cable force equals the mass multiplying the absolute acceleration.

$$d = \begin{pmatrix} d_x \\ d_y \\ d_z \end{pmatrix} = -m_L \begin{pmatrix} \ddot{x} + \ddot{r} \\ \ddot{y} + \ddot{s} \\ \ddot{z} + \ddot{\zeta} - g(\zeta/L) \end{pmatrix} \tag{7}$$

where m_L is the load mass and L is the cable length.

Since the load is suspended at the quadrotor's center of gravity, it only affects the quadrotor's translational motion while the rotational motion remains the same. That means the cable force only causes an acceleration on the quadrotor's x, y and z directions. Also, we assume the yaw angle is a constant value of zero by an independent controller. Combining Eqs. (1) – (4) and (7), we can obtain the interconnected dynamics shown in Eq. (8).

$$\begin{cases} \ddot{x} = \dfrac{\cos\phi \sin\theta}{m_q + m_L} U_1 - \dfrac{m_L}{m_q + m_L}\ddot{r} \\ \ddot{y} = -\dfrac{\sin\phi}{m_q + m_L} U_1 - \dfrac{m_L}{m_q + m_L}\ddot{s} \\ \ddot{z} = \dfrac{\cos\phi \cos\theta}{m_q + m_L} U_1 + \dfrac{m_L}{m_q + m_L}\dfrac{\ddot{r}r + \dot{r}^2 + \ddot{s}s + \dot{s}^2}{\zeta} \\ \qquad + \dfrac{m_L}{m_q + m_L}\dfrac{(\dot{r}r + \dot{s}s)^2}{\zeta^3} + \dfrac{m_L g \dfrac{\zeta}{L} + m_q g}{m_q + m_L} \\ \ddot{r} = (\zeta^4\ddot{x} - r\,\zeta^3\ddot{z} + rs\zeta^2\ddot{s} + (rL^2 - rs^2)\dot{r}^2 \\ +(rL^2 - r^3)\dot{s}^2 + 2\dot{r}\dot{s}r^2 s + rg\,\zeta^3)/((s^2 - L^2)\,\zeta^2) \\ \ddot{s} = (\zeta^4\ddot{y} - s\,\zeta^3\ddot{z} + rs\zeta^2\ddot{r} + (sL^2 - sr^2)\dot{s}^2 \\ +(sL^2 - s^3)\dot{r}^2 + 2\dot{r}\dot{s}s^2 r + sg\,\zeta^3)/((r^2 - L^2)\,\zeta^2) \end{cases} \tag{8}$$

Copyright © 2016 by ASME

Comparing to the original quadrotor dynamics in Eq. (5), we can treat the new r and s terms as external disturbances to the quadrotor. The details will be introduced in Section 3. In this way, we can simplify the uncertain suspended load problem back to the quadrotor control problem with external disturbances. Moreover, this disturbance can be regarded as bounded because the quadrotor payload is bounded.

3. CONTROL ALGORITHM DESIGN

The goal of the control system design is to make a quadrotor stabilize under the influence of an uncertain suspended load. In this section, the overall control scheme including an outer position controller and an inner attitude controller is firstly explained. Then we describe the SMDO-SMC controller and its implementation in the outer position control loop.

3.1 Overall Control Scheme

As we described in the previous section, we can treat the uncertain load as a bounded external disturbance to the quadrotor system. Thus, the quadrotor translational dynamic equations can be simplified to Eq. (9).

$$\begin{cases} \ddot{x} = \dfrac{\cos\phi \sin\theta}{m_q} U_1 + d_x \\ \ddot{y} = \dfrac{-\sin\phi}{m_q} U_1 + d_y \\ \ddot{z} = \dfrac{\cos\phi \cos\theta}{m_q} U_1 + g + d_z \end{cases} \tag{9}$$

where d_x, d_y and d_z are the disturbances caused by the load mass in Eq. (7). Also we assume these disturbances are bounded because we only consider the safety flight conditions, i.e., the payload mass should be inside the range between 0 and the maximum value M_{max}. In this way, our problem is simplified back to a normal quadrotor control problem. For our situation, we can define the problem as the form

$$\begin{cases} \dot{X} = F(X,t) + G(X,t)u + d \\ Y = H(X,t) \end{cases} \tag{10}$$

where the state $X = \{x, \dot{x}, y, \dot{y}, z, \dot{z}\}^T$, $Y = \{x, y, z\}^T$ and the disturbance $d = \{0, d_x, 0, d_y, 0, d_z\}^T$.

Based on these state equations, the overall control scheme is shown in Fig. 3. The outer position controller uses SMDO-SMC method which will be introduced in the next subsection. It determines the desired roll and pitch angles for the inner attitude controller. Then the PD technique is applied in the inner attitude controller to track two desired angles as well as the given yaw angle. This technique is a conventional one based on the error between the desired setpoint and measured value. As it has been discussed in many other works such as [29], we skip the details of this design in this paper. The quadrotor dynamics is based on Eqs. (5) and (9) while the load dynamics is depended on Eqs. (7) and (8). After being updated by control signals under the influence of the disturbance from the load dynamics, quadrotor's new states are sent to the load dynamics and the position controller.

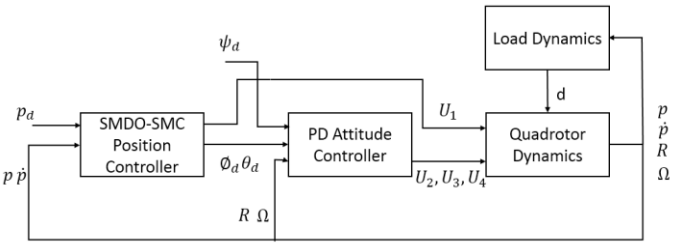

Figure 3: Overall Control Scheme. According to the expected and current position, the SMDO-SMC position controller determines the desired roll and pitch angles for the PD controller to track. Based on two controllers' control signal, the quadrotor dynamics block computes the states, which are used by the load dynamics and the position controller.

3.2 SMDO-SMC Controller

Since the system in Eq. (10) can be completely feedback linearizable, it can be changed to a regular form as in [22]. First we introduce the tracking error as $e = y_d - y$ as well as sliding variable σ and external disturbances as

$$\sigma_i = e_i^{(r_i-1)} + c_{i,r_i-2} e_i^{(r_i-2)} + \cdots + c_{i,1} e_i^{(1)} + c_{i,0} e_i \tag{11}$$

$$\Psi_i = \Psi_i^0 + \Delta\Psi_i \tag{12}$$

where Ψ_i means the external disturbance, Ψ_i^0 is the known part while $\Delta\Psi_i$ represents the bounded uncertainties ($||\Delta\Psi_i|| \le L_i$).

If defining the control input as $\tilde{u}_i = \tilde{u}_{i,0} + \tilde{u}_{i,1}$ and using $\tilde{u}_{i,0}$ to compensate the known part ($\tilde{u}_{i,0} = \Psi_i^0$), then we know the control deriving $\dot{\sigma} = \Delta\Psi_i - \tilde{u}_{i,1}$ to zero will be equal to the disturbance term. The SMDO theory defines the auxiliary sliding variables s_i and z_i such that

$$\begin{cases} s_i = \sigma_i + z_i \\ \dot{z}_i = \tilde{u}_{i,1} - v_i \\ \dot{s}_i = \Delta\Psi_i - v_i \end{cases} \tag{13}$$

Then, $v_i = (\rho_i + L_i) sgn(s_i)$ is the control deriving s_i to zero and maintain s_i there for all subsequent time. However, it shows high-frequency switching, so we use a low pass filter in Eq. (14) to lower its frequency.

$$\hat{v}_{i,eq} = 1/(1 + \beta_i s) v_i \tag{14}$$

β_i should be chosen carefully and it is recommended to satisfy $\lim_{\beta \to 0} \frac{\Delta t}{\beta} = 0$ in [22]. Till now, we have finished the estimation of the unknown disturbance term $\Delta\Psi_i$ and the resultant control $\tilde{u}_i = \tilde{u}_{i,0} + \hat{v}_{i,eq}$ completely compensates for the system dynamics. However, a final control term needs to be added to drive σ_i to zero and satisfy the sliding model existence condition. Therefore, the final SMC-SMDO control signal is

$$\tilde{u}_i = \tilde{u}_{i,0} + \hat{v}_{i,eq} + K_{0,i}\sigma_i \tag{15}$$

where $K_{0,i} > 0$ is chosen to ensure fast reaching of the sliding surface by σ as soon as the disturbance is estimated and compensated (i.e. the convergence of σ_i cannot be faster than that of s_i).

Copyright © 2016 by ASME

3.3 Implementation of SMDO-SMC Based Control on Quadrotor

First, we define a tracking error between the position command profile and the actual position as $e_1 = [p_d - p]^T = [x_d - x, y_d - y, z_d - z]^T$ and sliding variable $\sigma_1 = [\sigma_x, \sigma_y, \sigma_z]^T$ as $\sigma_{1,i} = \dot{e}_{1,i} + C_{i,0}^1 e_{1,i}$, where the gain $C_{i,0}^1$ is chosen such that the tracking error, e_1, exhibits the desired behavior in the sliding mode. Then based on the results in section 3.2, we can design the final SMDO-SMC control signal as

$$\begin{cases} \sigma_{1,i} = \dot{e}_{1,i} + C_i^1 e_{1,i} \\ s_{1,i} = \sigma_{1,i} + z_{1,i} \\ \dot{z}_{1,i} = \tilde{u}_{1,i} - v_{1,i} \\ v_{1,i} = (\rho_{1,i} + L_{1,i}) sgn(s_{1,i}) \\ \hat{v}_{eq,1,i} = \dfrac{1}{(\beta_i s + 1)^2} v_{1,i} \\ u_{1,i} = \Psi_{0,i}^1 + \hat{v}_{eq,1,i} + K_i^1 \sigma_{1,i} \end{cases} \quad (16)$$

where, C_i^1, $\rho_{1,i}$, β_i and K_i^1 are human chosen parameters. They should be non-negative. After obtaining the control signal $u_1 = [u_{1,x}, u_{1,y}, u_{1,z}]^T$, we can use Eq. (17) to compute the thrust and commanded roll and pitch angles, which will be used by the quadrotor dynamics calculation and the inner PD attitude controller.

$$\begin{cases} U_1 = \|m(u_1 - g e_3)\| \\ \phi_d = \text{asin}\left(-\dfrac{m_q}{U_1} u_{1y}\right) \\ \theta_d = \text{asin}\left(\dfrac{m_q}{U_1 \cos \phi_d} u_{1x}\right) \end{cases} \quad (17)$$

4. NUMERICAL SIMULATION

4.1 Simulation Setup

In this paper, all simulations are completed in MATLAB/Simulink. The parameters of the quadrotor system in Eqs. (1) – (4) and (8) are shown in Table 1.

Table 1: Quadrotor Simulation Parameters

Parameter	Value	Description
I_x, I_y	7.5*10^(-3) kg/m^2	Quadrotor moment of inertia around X axis and Y axis
I_z	1.3*10^(-2) kg/m^2	Quadrotor moment of inertia around Z axis
m_q	1kg	Quadrotor mass
K_b	3.13*10^(-5)	Thrust factor for F_i
K_d	7.5*10^(-7)	Drag factor for Q_i
l	0.25m	Distance between the rotor center and quad center
L	0.5m	The cable length
M_{max}	0.6kg	Maximum payload mass

Four cases with different load masses are discussed to compare the impacts of the mass uncertainty on the quadrotor system. As mentioned by most quadrotor manufacturers and designers, the quadrotor behaves inappropriately or unreasonably if the payload mass exceeds its maximum capacity. Given this situation, it is meaningless to evaluate our controller performance which is designed for normal and reasonable flights. Therefore, we only consider the load mass in the range [0, 0.6kg]. According to the design theory in Section 3.2, we keep the known part Ψ_i^0 in the disturbance to be $0.3g$ so that the unknown bound will be $\|\Delta\Psi_i\| \leq L_i = 0.3g$. To test its robustness, we simulated four cases with the load masses of 0.01kg, 0.2kg, 0.3kg and 0.5kg, so the corresponding absolute uncertainties are nearly 0.3kg, 0.1kg, 0kg and 0.2kg. These are four typical situations including the minimum, medium, maximum values in the uncertainty range of $[0,0.3\text{kg})$. The reason using 0.01kg instead of 0kg is that the latter makes the cable force negligible which violates the assumption (4). Since both controllers are initially designed for a 0.3kg mass, the control performance should decrease as the uncertainty increases. In other words, a 0.3kg load mass with zero uncertainty should be ideal case while a 0.01kg load mass (nearly 0.3kg uncertainty) should be worst case.

In each case, we define the quadrotor's initial position is $[0,0,1]^T$. The initial load's x and y positions are both 0.2m, which means the interconnected system is not at equilibrium and the load should begin moving at first due to the gravity force. Our control goal is to stabilize the interconnected system at the end, i.e., the final position of the quadrotor should still be $[0,0,1]^T$ and the final load's position should be $[r, s, \zeta]^T = [0,0,0.5]^T$. Since the altitude z and yaw angle ψ has no coupling with other states and can remain the desired value precisely, the control performance is evaluated on the quadrotor's x, y positions, the roll, pitch angles and the load's x, y positions. The control parameters are shown in Table 2. Note these parameters are not changeable during four cases and they are initially designed for the 0.3kg load mass.

Table 2: Control Parameters

Parameter	Value	Description
K_{px}, K_{py}	3	Proportional gain for x and y
K_{pz}	10	Proportional gain for z
K_{dx}, K_{dy}	15	Derivative gain for x and y
K_{dz}	8	Derivative gain for z
K_{pp}, K_{pt}	50	Proportional gain for ϕ and θ
K_{pps}	20	Proportional gain for ψ
K_{dp}, K_{dt}	20	Derivative gain for ϕ and θ
K_{dps}	15	Derivative gain for ψ
C_i^1	5	σ related parameter in Eq. (16)
$\rho_{1,i}$	0.1	v related parameter in Eq. (16)
β_i	0.01	Low pass filter frequency in Eq. (16)
K_i^1	10	u related parameter in Eq. (16)

Copyright © 2016 by ASME

4.2 Simulation Results

Case 1: The absolute mass uncertainty is 0kg.

This case is also known as a 0.3kg load mass. Fig. 4(a) – (d) shows the control performance of a PD controller and the SMDO-SMC method respectively.

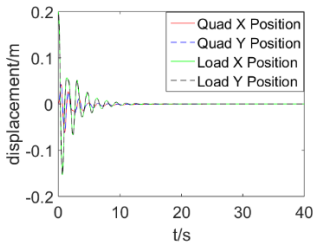

(a): The position of the PD controller

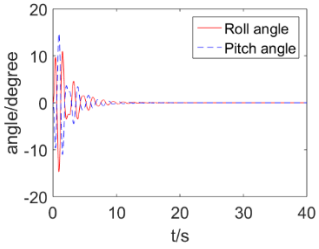

(b): The angle of the PD controller

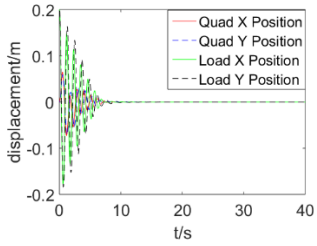

(c): The position of SMDO-SMC

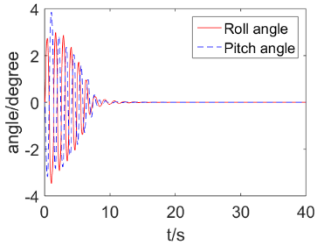

(d): The angle of SMDO-SMC

Figure 4: Two control performances with 0.3kg load mass. The SMDO-SMC method stabilizes at around 12s with 4-degree overshoot while the PD controller stabilizes at around 14s with 14-degree overshoot.

From this figure, the stabilization time of SMDO-SMC is at about 12s which is 2 seconds shorter than the PD controller's 14s. The angle response amplitude of SMDO-SMC remains in the range of [-4,4] degrees while the PD controller is in [-15,15] degrees. Both the load position displacement responses are between -0.2m and 0.2m while the quadrotor position responses are close to each other in [-0.1,0.1] meters. However, the load position amplitude of SMDO-SMC is about 0.05-0.1m higher than the PD controller during the first 4 seconds. This is because SMDO-SMC needs some time to estimate the external disturbance uncertainty first. As this uncertainty is estimated out and compensated gradually, the system begins to converge fast. This can also be reflected by a time period of 5s-10s. In terms of the stabilization time and attitude maintaining, SMDO-SMC has a better performance than a PD controller.

Case 2: The absolute mass uncertainty is 0.1kg.

This case is also known as a 0.2kg load mass. The control performance with this small uncertainty is shown in Fig. 5(a) – (d) below.

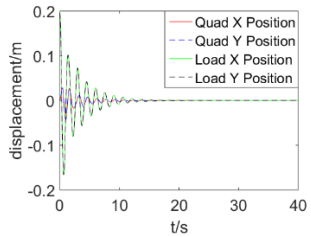

(a): The position of the PD controller

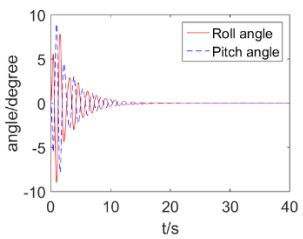

(b): The angle of the PD controller

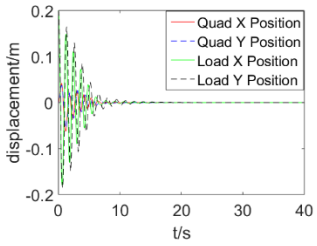

(c): The position of SMDO-SMC

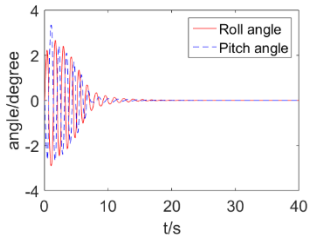

(d): The angle of SMDO-SMC

Figure 5: Two control performances with 0.2kg load mass. The SMDO-SMC method stabilizes at around 13s with 4-degree overshoot while the PD controller stabilizes at around 17s with 8-degree overshoot.

From Figure 5, the SMDO-SMC control performance almost maintains. The only difference is that the stabilization time is one second longer than case 1. Since the uncertainty is not big, it can still be addressed by the PD controller. Thus, the PD control performance also keeps while the stabilization time is 3 seconds later than case 1. Another important difference here is a decrease of 6 degrees in the angle overshoot. The reason is that the load mass in this case is smaller than case 1. If starting from the same initial angle, the smaller mass correspondingly has a smaller overshoot. In contrast, the SMDO-SMC angles are close to case 1. Considering the angle amplitude, SMDO-SMC deals with the uncertainty better than a PD controller.

Case 3: The absolute mass uncertainty is 0.2kg.

This case is also known as a 0.5kg load mass. The mass uncertainty begins increasing and its impacts can be seen in Fig. 6 (a) – (d).

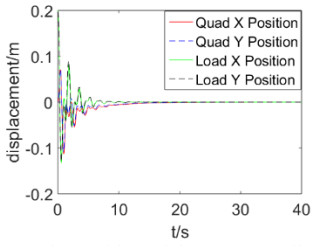

(a): The position of the PD controller

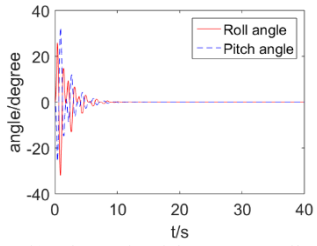

(b): The angle of the PD controller

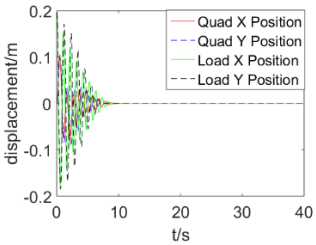

(c): The position of SMDO-SMC

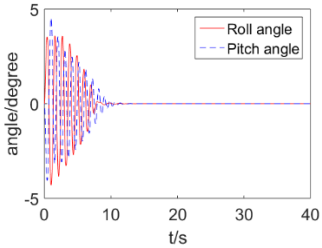

(d): The angle of SMDO-SMC

Figure 6: Two control performances with 0.5kg load mass. The SMDO-SMC method stabilizes at around 13s with 5-degree overshoot while the PD controller stabilizes at around 21s with 30-degree overshoot.

In this case, the SMDO-SMC control performance is still close to the first two cases. The angle overshoot increases by about 1 degree. On the other hand, the PD controller stabilizes 8 seconds later than SMDO-SMC with a 30-degree angle overshoot. According to the stabilization time and angle overshoot, the difference of addressing the uncertainty between two controllers becomes bigger.

Copyright © 2016 by ASME

Case 4: The absolute mass uncertainty is nearly 0.3kg.

Since we assume the cable is massless, we cannot make the payload mass to be 0kg. If so, the load position will be meaningless. As a result, we use 0.01kg instead to test the approximate maximum bound limit. Because the PD control parameters are designed for a 0.3kg payload, this uncertainty is large enough to make the controller unstable. It is indicated by the termination of the Simulink simulation, in which the load's positions r and s exceed the range of [0,0.5] violating the cable length constraints. Therefore, we only show the SMDO-SMC control performance in Fig. 7.

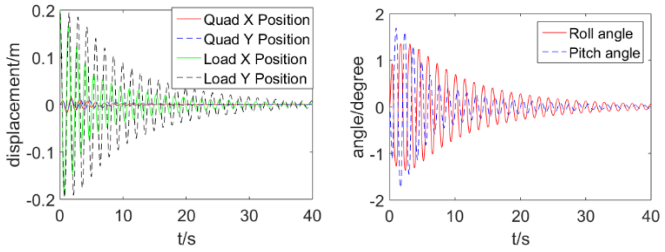

(a): The position (b): The angle

Figure 7: The control performance of SMDO-SMC. The stabilization time is over 40s, but it still shows convergence.

From the above figure, the quadrotor's position still stabilizes and maintains in a small range of [-0.02,0.02] meters. But the load's position and quadrotor's attitude converge slower. The reason is the payload's light weight. Its impact on the quadrotor is not significant any more, which violates the assumption (4). As seen in Fig. 7 (b), however, the attitude almost changes in the range of [-1,1] degrees. If allowing some deviations for the quadrotor, 20s can be considered as the stabilization time. Anyway, SMDO-SMC outperforms the PD controller with regard to robustness against large uncertainties.

5. CONCLUSION

In this paper, we have investigated the influences of uncertain load masses on the quadrotor. This uncertainty is proved to have a notable impact on the quadrotor's stability and the impact gets stronger as the uncertainty increases. If the uncertainty is large enough, it can lead some controllers like the PD controller to fail. The better performance of SMDO-SMC than the PD controller verifies the importance of the controller's robustness against disturbances. Therefore, a controller with a strong robustness against disturbances is a better choice for the practical uncertain load transportation. In the next stage, we want to verify the simulation results in the real quadrotor systems. Also, we want to include a take-off or landing phase rather than just mid-air hovering.

NOMENCLATURE

$\boldsymbol{p}$	quadrotor position
$\boldsymbol{v}$	quadrotor linear translational velocity
m_q	quadrotor mass
m_L	load mass
$\boldsymbol{g}$	acceleration of gravity
$\boldsymbol{R}$	rotation matrix from frame {B} to frame {W}
$\boldsymbol{f}$	upwards thrust
$\boldsymbol{\Omega}$	angular velocity
$\mathbf{S}(\cdot)$	skew-symmetric operator
$\mathbf{I}$	body-fixed inertia matrix
$\boldsymbol{T}$	applied moments
r	load x position
s	load y position
ζ	load z position
L	cable length
σ	sliding variable
Ψ_i	external disturbance
Ψ_i^0	known part of Ψ_i
$\Delta\Psi_i$	bounded uncertainties
s_i	auxiliary sliding variables
z_i	auxiliary sliding variables
$\hat{v}_{eq}$	estimation of $\Delta\Psi$
C_i^1	σ related parameter
$\rho_{1,i}$	v related parameter
β_i	low pass filter frequency
K_i^1	u related parameter

REFERENCES

[1] Bernard, M. and Kondak, K., 2009, "Generic slung load transportation system using small size helicopters," In *International Conference on Robotics and Automation*, pp. 3258-3264.

[2] Bernard, M., Kondak, K., Maza, I., and Ollero, A., 2011, "Autonomous transportation and deployment with aerial robots for search and rescue missions," In *Journal of Field Robotics*, Vol. 28, Issue 6, pp. 914-931.

[3] Palunko, I., Cruz, P., and Fierro, R., 2012, "Agile Load Transportation: Safe and Efficient Load Manipulation with Aerial Robots," in *IEEE Robotics Automation Magazine*, Vol. 19, pp. 69-79.

[4] Palunko, I., Fierro, R., and Cruz, P., 2012, " Trajectory Generation for Swing-free Maneuvers of a Quadrotor with Suspended Payload: A dynamic programming approach," in *2012 IEEE International Conference on Robotics and Automation (ICRA)*, pp. 2691-2697.

[5] Goodarzi, F. A., Lee, D., and Lee, T., 2014, "Geometric Stabilization of Quadrotor UAV with a Payload Connected by Flexible Cable," in *American Control Conference (ACC)*, pp. 4925-4930.

[6] Michael, N., Fink, J., and Kumar, V., 2010, "Cooperative Manipulation and Transportation with Aerial Robots," in *Autonomous Robots*, New York: Springer-Verlag.

[7] Lindsey, Q., Mellinger, D., and Kumar, V., 2011, "Construction of Cubic Structures with Quadrotor Teams," in *Autonomous Robots,* Vol. 33, Issue 3, pp. 323-326.

[8] Sreenath, K., Michael, N., and Kumar, V., 2013, "Trajectory Generation and Control of a Quadrotor with a Cable-suspended Load - a Differentially-flat Hybrid System," in *IEEE International Conference on Robotics and Automation (ICRA)*, pp. 4888–4895.

Copyright © 2016 by ASME

[9] Sreenath, K., Lee, T., and Kumar, V., 2013, "Geometric Control and Differential Flatness of a Quadrotor UAV with a Cable suspended Load," in *IEEE 52nd Annual Conference on Decision and Control (CDC)*, pp. 2269–2274.

[10] Palunko, I., and Fierro, R., 2011, "Adaptive Control of a Quadrotor with Dynamic Changes in the Center of Gravity," in *Proceedings of the 18th IFAC World Congress*, pp. 2626–2631.

[11] Crousaz, C. de, Farshidian, F., and Buchli, J., 2014, "Aggressive Optimal Control for Agile Flight with a Slung Load," In *IROS 2014 Workshop on Machine Learning in Planning and Control of Robot Motion*.

[12] Faust, A., Palunko, I., Cruz, P., Fierro, R., and Tapia, L., 2013, "Learning Swing-free Trajectories for UAVs with a Suspended Load," in *IEEE International Conference on Robotics and Automation (ICRA)*, pp. 4902–4909.

[13] Trachte, J. E., Gonzalez Toro, L. F., and McFadyen, A., 2015, "Multi-rotor with Suspended Load: System Dynamics and Control Toolbox," in *IEEE Aerospace Conference*, pp. 1-9.

[14] Sreenath, K., and Kumar, V., 2013, "Dynamics, Control and Planning for Cooperative Manipulation of Payloads Suspended by Cables from Multiple Quadrotor Robots," In *Robotics: Science and Systems (RSS)*.

[15] Mellinger, D., Shomin, M., Michael, N., and Kumar, V., 2013, "Cooperative Grasping and Transport Using Multiple Quadrotors," In *Distributed autonomous robotic systems*, pp. 545-558.

[16] Wu, G., and Sreenath, K., 2014, "Geometric Control of Multiple Quadrotors Transporting a Rigid-body Load," In *IEEE 53rd Annual Conference on Decision and Control (CDC)*, pp. 6141-6148.

[17] Min, B., Hong, J., and Matson, E. T., 2011, "Adaptive Robust Control (ARC) for an Altitude Control of a Quadrotor Type UAV Carrying an Unknown Payloads," in *11th International Conference on Control, Automation and Systems (ICCAS)*, pp. 1147-1151.

[18] Dai, S., Lee, T., and Bernstein, D. S., 2014, "Adaptive Control of a Quadrotor UAV Transporting a Cable-Suspended Load with Unknown Mass," In *IEEE 53rd Annual Conference on Decision and Control (CDC)*, pp. 6149-6154.

[19] Lee, D., Kim, J. H., and Sastry, S., 2009, "Feedback Linearization vs. Adaptive Sliding Mode Control for a Quadrotor Helicopter," In *International Journal of Control, Automation and Systems*, Vol. 7, Issue 3, pp. 419-428.

[20] Madani, T., and Benallegue, A., 2007, "Sliding Mode Observer and Backstepping Control for a Quadrotor Unmanned Aerial Vehicles," In *American Control Conference*, pp. 5887-5892.

[21] Bouadi, H., and Tadjine, M., "Nonlinear Observer Design and Sliding Mode Control of Four Rotors Helicopter," In *World Academy of Science, Engineering and Technology*, Vol. 1, Issue 7, pp. 329-334.

[22] Bensnard, L., Shtessel, Y. B., Landrum, B., 2012, "Quadrotor Vehicle Control Via Sliding Mode Controller Driven by Sliding Mode Disturbance Observer," in *Journal of the Franklin Institute*, Vol. 349, Issue 2, pp. 658-684.

[23] Sadr, S., Ali S., Moosavian, A., and Zarafshan, P., 2014, "Dynamics Modeling and Control of a Quadrotor with Swing Load," In *Journal of Robotics*, Vol. 2014, Article ID 265897, 12 pages.

[24] Mahony, R., Kumar, V., and Corke, P., 2012, "Modeling, Estimation, and Control of Quadrotor," In I*EEE Robotics and Automation magazine,* Vol. 19, pp. 20-32.

[25] Klausen, K, Fossen, T. I., and Johansen, T. A., 2015, "Nonlinear Control of a Multirotor UAV with Suspended Load," In *International Conference on Unmanned Aircraft Systems,* pp. 176-184.

[26] Bouabdallah, S., Murrieri, P., and Siegwart, R., 2004, "Design and Control of an Indoor Micro Quadrotor," In *International Conference on Robotics and Automation,* pp. 4393-4398.

[27] Bouabdallah, S., and Siegwart, R., 2007, "Full Control of a Quadrotor," In *IEEE/RSJ International Conference on Intelligent Robots and Systems*, pp. 153-158.

[28] Hehn, M., and D'Andrea, R., 2011, "A Flying Inverted Pendulum," In *International Conference on Robotics and Automation*, pp. 763-770.

[29] Li, J., and Li, Y., 2011, "Dynamic Analysis and PID Control for a Quadrotor," In *International Conference on Mechatronics and Automation (ICMA)*, pp. 573-578.

Copyright © 2016 by ASME

View publication stats